Post-collision interactions and the polarization effect in (e, 2e) collisions of helium

Zang Shuang-Shuang(臧爽爽) and Ge Zi-Ming(葛自明)†

Department of Physics, East China University of Science and Technology, Shanghai 200237, *China*

(Received 16 September 2011; revised manuscript received 8 December 2011)

A modified distorted-wave Born approximation (DWBA) method is used to calculate the triple differential cross sections (TDCSs) in a coplanar asymmetric geometry for the electron impact single ionization of a He ($1s^2$) atom at intermediate and lower energies. The post-collision interaction and the polarization effect in (e, 2e) collisions of helium are considered in the calculations. The polarization potentials from the damping method and density functional theory (DFT) are compared. Theoretical results are compared with the recent experimental data.

Keywords: post collision interactions, polarization potential, density-functional theory (DFT), distorted wave Born approximation (DWBA)

PACS: 34.80.Dp **DOI:** 10.1088/1674-1056/21/7/073403

1. Introduction

The (e, 2e) experiments have revealed a wealth of new information about the single ionization (SI) of atoms and molecules in a very wide energy range from threshold up to the relativistic regime.[1−3] It has become a well-established, powerful tool for investigating very fine details both of the target structure and of the dynamics of the ionization process.[4−6] Therefore, in recent years, numerous studies have been performed on (e, 2e) electron-impact ionization processes.[7−9] The most detailed possible information about the mechanism of ionization reactions or about the structure of the target is provided by the triple differential cross sections (TDCS) obtained by angular correlation (e, 2e) experiments.[10−12]

Surprisingly, Lahmam–Bennani[13] reported on the experimental TDCS results for low-energy electron impact ionization of He($1s^2$) in coplanar asymmetric geometry. The theoretical TDCS results do not give an entirely satisfactory description of the experimental results in the overall shape and magnitude of the TDCS. It is seen that the theory behaves less and less well as energy decreases. The discrepancy between the standard distorted wave Born approximation (DWBA) and the experimental data is probably due to the neglecting of the higher-order electron–electron correlations.[14,15] Recently Dürr *et al.*[16] studied single ionization of helium by 102 eV electron impact with an advanced reaction microscope, fully differential cross sections for asymmetric scattering geometry obtained covering a large range of emission angles. Theoretical predictions from a three-Coulomb (3C) wavefunction model, a convergent close-coupling (CCC) calculation and the time-dependent close-coupling (TDCC)[17] approach were used to calculate the cross sections, and different degrees of agreement were obtained with the experimental data, which suggested a strong sensitivity to the details of the models. However, none of these methods could reproduce the experimental data completely.

The three primary physical effects that are likely to cause the disagreement between experiment and theory are post-collision interactions (PCI), charge cloud polarization, and electron exchange. At intermediate and low incident energies, the description of the ionization process becomes very complex, as it involves short- and long-range interactions, including polarization, capture, and exchange processes. All of these differences imply that there are some other mechanisms that have not been treated in these (e, 2e) reactions. Thus accurate theoretical calculations are necessary in order to understand the interaction and collision process correctly.

In this paper we extend the model proposed by Whelan *et al.*[18] and add another potential $V_{\rm p}$ via the density functional theory (DFT) for He. The best currently available method of treating PCI in a first-

†Corresponding author. E-mail: geziming@ecust.edu.cn

© 2012 Chinese Physical Society and IOP Publishing Ltd

order calculation is realized through the Gamow factor $N_{\rm ee}$.[19] We aim at showing the influences of the PCI and polarization potential on the calculated TDCS of He($1s^2$) target. In order to test the validity of our model, we calculate the TDCS with the incident energies of 50 eV and 102 eV for a He atom in an asymmetric geometry. The calculated results are compared with those obtained by the standard DWBA and the experimental data.

2. Theory

The TDCS in the DWBA including the Gamow factor $N_{\rm ee}$ is given by

$$\frac{{\rm d}^3\sigma}{{\rm d}\Omega_{\rm f}\,{\rm d}\Omega_{\rm s}\,{\rm d}E_0} = N_{\rm ee}(2\pi)^4\frac{k_{\rm f}k_{\rm s}}{k_0}\sum_{\rm av}|\langle \boldsymbol{k}_{\rm f}\boldsymbol{k}_{\rm s}|\,T\,|\alpha\boldsymbol{k}_0\rangle|^2. \tag{1}$$

The notation $\sum\limits_{\rm av}$ represents a sum over the final states and average over the initial magnetic and spine degeneracy states. In our calculations, atomic units ($h = m_{\rm e} = e = 1$) are used.

The T-matrix element which represents the ionization amplitude is conveniently written in terms of distorted waves as:

$$\langle \boldsymbol{k}_{\rm f}\boldsymbol{k}_{\rm s}|\,T\,|\alpha\boldsymbol{k}_0\rangle = \left\langle \chi^{(-)}(\boldsymbol{k}_{\rm f})\chi^{(-)}(\boldsymbol{k}_{\rm s})\right|\,v_{\rm fs}\left|\alpha\chi^{(+)}(\boldsymbol{k}_0)\right\rangle, \tag{2}$$

where $\nu_{\rm fs}$ is the interaction potential between the fast electron and the slow electron, $\left|\chi^{(+)}(\boldsymbol{k}_0)\right\rangle$, $\left|\chi^{(-)}(\boldsymbol{k}_{\rm f})\right\rangle$ and $\left|\chi^{(-)}(\boldsymbol{k}_{\rm s})\right\rangle$ are the distorted waves in different asymptotic conditions. The superscripts "+" and "–" refer to the incident and outgoing wave, respectively.

We neglect spin-orbit coupling and treat the core as being infinitely massive. The Gamow factor $N_{\rm ee}$ is defined as[19]

$$N_{\rm ee} = \frac{\gamma}{{\rm e}^{\gamma}-1},\quad \left(\gamma = \frac{2\pi}{|\boldsymbol{k}_{\rm f}-\boldsymbol{k}_{\rm s}|}\right). \tag{3}$$

The fundamental form of the short-range correlation plus the long-range polarization potential may be approximated by means of the DFT and the damping polarization potential as follows:

$$V_{\rm p}(r) = \begin{cases} V_{\rm p}^{\rm DFTCP}(r), & r \le r_0, \\ V_{\rm p}^{\rm damp}(r), & r > r_0. \end{cases} \tag{4}$$

Here, $V_{\rm p}^{\rm DFTCP}$[20] is the correlation polarization potential from DFT (DFTCP), and $V_{\rm p}^{\rm damp}$ is the damping polarization potential. DFTCP can be nicely connected with $V_{\rm p}^{\rm damp}$[21] at $r_0 = 5.6\ a_0$.

3. Results and discussion

We present the $V_{\rm p}^{\rm damp}$ for a He atom and compare it with the correlation polarization potential $V_{\rm p}^{\rm DFTCP}$ in Fig. 1. One clearly sees from the figure that although $V_{\rm p}^{\rm damp}$ provides a good description at large distances, it markedly overestimates polarization effects as $r_{\rm e}$, the distance of the electron from the atomic nucleus, becomes smaller and diverges near the origin of the field of forces. Fortunately, the present description of correlation forces modifies the traditional polarization potential and describes short-range correlation via an effective, non-adiabatic interaction which vanishes at the origin of the force field. Thus, the non-adiabatic correlation effects resulting from the penetration of the electron must be taken into account.

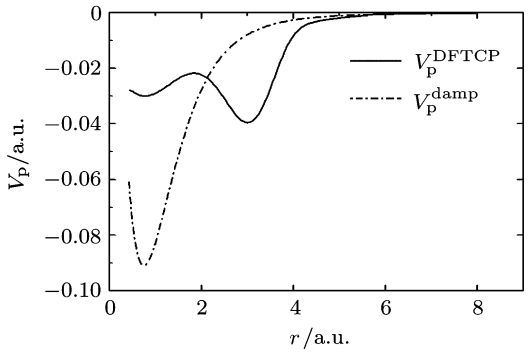


Fig. 1. Computed correlation polarization potential $V_{\rm p}$ for He target.

Figures 2 and 3 show the calculated TDCSs of He($1s^2$) in an asymmetric geometry. The impact energy of 50 eV is chosen, and the polar angle of the fast electron is settled at $\theta_{\rm f} = -20°$ and $\theta_{\rm f} = -30°$, respectively. The only variable parameter is the polar angle $\theta_{\rm s}$ of the ejected electron, which is scanned from 0° to 360°. We show the TDCSs in coplanar asymmetric geometry with different DWBA approximations: (a) the standard DWBA calculation; (b) the DWBA1 calculations using $N_{\rm ee}$ factor and the damping polarization $V_{\rm p}^{\rm damp}$; (c) the DWBA2 calculations using $N_{\rm ee}$ factor and the correlation polarization $V_{\rm p}$ from DFT. The experimental data are not absolute values,[13] so only shapes can be compared. Hence we normalize the relative experimental data to the present calculated results using the standard DWBA. The normalized wave function of the target is approximated by the Hartree–Fock (HF) independent-electron orbital model.

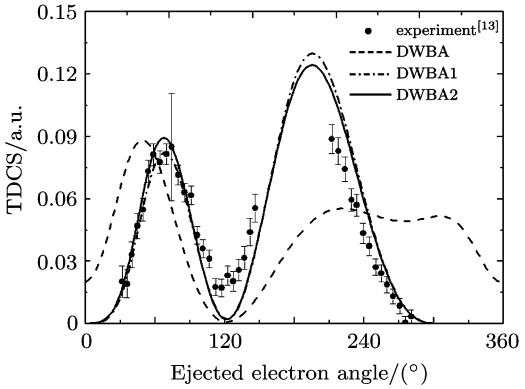


Fig. 2. TDCSs for the He($1s^2$) ionization, E_0=50 eV, E_s=10 eV, $\theta_f = -20°$.

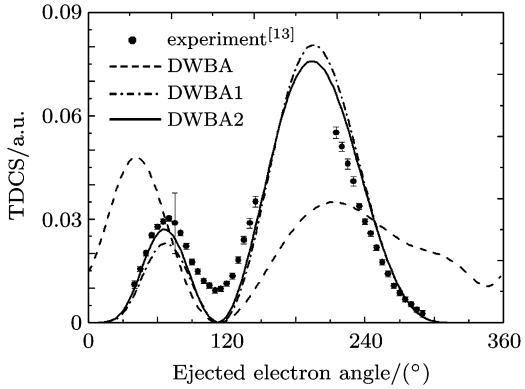


Fig. 3. The same as Fig. 2 but for E_0=50 eV, E_s=10 eV, $\theta_f = -30°$.

The calculated TDCSs of He($1s^2$) in coplanar asymmetric geometry with the polar angles of the fast electron settled at $-20°$ are presented in Fig. 2. The theoretical results calculated using the modified DWBA and THFA methods are compared with the experimental data in Ref. [13]. We can see from Fig. 2 that the structures of the angular distribution of the ejected electrons are composed of two lobes, binary and recoil. The calculation with the standard DWBA is hardly satisfactory in reproducing the experimental findings and gives poor description of the experimental results in the overall shape, magnitude of the TDCS, and angular position of the binary peak. The calculated binary lobe and recoil lobe with the standard DWBA are rather asymmetric with respect to K. The angular position of binary peak from the theoretical calculation using the standard DWBA is 41.5°, whereas the angular position of the experimental result is about 70°. The ratio of the binary-to-recoil peak intensity is also poorly predicted by the standard DWBA.

Calculations by using the DWBA1 give a good description of the experimental results in the overall shape. For the binary peak, the calculation by using the DWBA1 with considering the Gamow factor N_{ee} and polarization potential V_p^{damp} gives an angular position of about 66°, which is close to the experimental result 70°. Replacing polarization potential V_p^{damp} with the polarization potential V_p, which contains both the damping polarization potential V_p^{damp} and the DFT polarization potential V_p^{DFTCP}, a better improvement is achieved. The magnitude of the binary peak is enhanced while the magnitude of the recoil peak is reduced, which altogether made the ratio of the binary to recoil peak much closer to the experimental results. All these improvements indicate that the Gamow factor N_{ee} and polarization potential V_p are quite important for the calculation of the TDCS of the (e, 2e) collisions of He.

The calculated TDCSs of He($1s^2$) with the polar angle of the fast electron settled at $-30°$ are shown in Fig. 3. We can see that the calculation with standard DWBA not only incorrectly reproduces the experimental findings but also gives a poor description of the experimental results in the overall shape. The calculation by using the DWBA1, and considering the Gamow factor N_{ee} and polarization potential V_p^{damp} gives the increased magnitude of recoil peak and the reduced binary peak, presenting an angular shift of about 17.5°. With the DWBA2 calculation, in which the Gamow factor N_{ee} and the polarization potential V_p are taken into consideration, we obtain more improved theoretical results, which makes not only the magnitude of the recoil peak lower, but also the magnitude of the binary peak higher. In fact, in the energy range shown here, the traditional DWBA prediction is unable to correctly reproduce the experimental data. Most of the deviations between the theoretical and the experimental data can be accounted for by taking the PCI and the polarization into consideration in the low-energy incident electron (e, 2e) reactions.

Figures 4 and 5 contain the calculated TDCSs of He($1s^2$) with chosen impact energy of 102 eV, and the polar angle of the fast electron set at $\theta_f = -10°$ and $\theta_f = -20°$ respectively. We present the results of TDCS for He($1s^2$) versus the scattering angle of the emitted electron in Fig. 4. We can see that the recoil peak observed grow while the binary peak appears to decrease in our calculations when the incident energy decreases from 102 eV to 50 eV. The standard DWBA calculation presents an obvious angular shift towards smaller angles for about 16° in the binary region. It also gives an unexpected higher binary peak

and a lower recoil peak, which together induce a terrible binary-to-recoil peak ratio. Since PCI and the damping polarization potential are taken into consideration, the DWBA1 calculation improves the magnitude of the recoil peak obviously but underestimates the binary peak. Surprisingly, we find that the agreement between the DWBA2 calculation and the measurement is generally very good. The binary-to-recoil peak ratios are 1.04 and 0.93 in DWBA2 calculation and DWBA1 calculation, respectively, which is 1.08 experimentally.

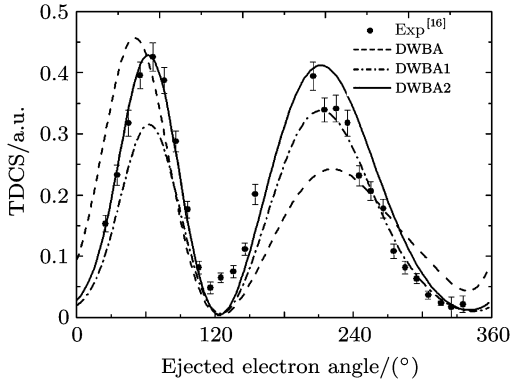


Fig. 4. The same as Fig. 2 but for E_0=102 eV, E_s=10 eV, $\theta_f = -10°$.

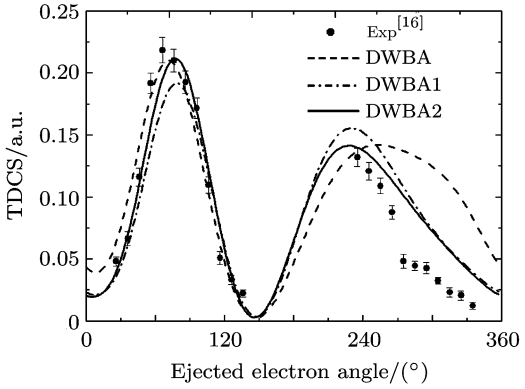


Fig. 5. The same as Fig. 2 but for E_0=102 eV, E_s=5 eV, $\theta_f = -20°$.

The calculated TDCSs for He($1s^2$) at $\theta_f = -20°$ are presented in Fig. 5. The standard DWBA calculation gives good agreement with experimental results in the binary region but fails to reproduce the recoil peak structure. The theoretical results obtained using the DWBA method do not give an entirely satisfactory description of the recoil peak structure when the ejected electron energy decreases from 10 to 5 eV. The theoretical calculation of TDCS at low energy regime requires a careful treatment of both initial and final states. As can be seen from the comparison between the DWBA1 calculation and the DWBA2 calculation, the correlation-polarization potential V_p is able to modify the damping polarization potential V_p^{damp} successfully.

4. Conclusion

Calculations of the triple differential cross section for the electron impact ionization of a Helium ($1s^2$) atom in a coplanar asymmetric geometry, using modified DWBA, are reported. The present calculations show that the N_{ee} factor and the polarization effect well predict the most detailed possible information about the TDCSs for the intermediate and low energy incident electrons (e, 2e) reactions. The mechanism of PCI and the relation in the final states in (e, 2e) reactions are partially included in the Gamow factor N_{ee} and the polarization potentials. Consequently, in the intermediate and low energy (e, 2e) reactions, the N_{ee} factor and the polarization potential must be incorporated into the DWBA calculation. Although in the present work the results of the standard DWBA calculation are successfully modified, a small discrepancy between these calculations and the experimental results still exists, which requires further investigation of (e, 2e) processes on this target. We strongly believe that the inclusion of PCI, higher-order projectile-target-core interaction and better treatment of polarization may improve the trends of TDCS.

References

[1] Stevenson M A, Hargreaves L R, Lohmann B, Bray I, Fursa D V, Bartschat K and Kheifets A 2009 *Phys. Rev.* A **79** 012709

[2] Hu X Y and Zhou Y J 2008 *Phys. Lett.* A **372** 4809

[3] Sun S Y, Jia X F, Miao X Y, Zhang J F, Xie Y, Li X W and Shi W Q 2009 *Chin. Phys.* B **18** 2744

[4] Macek J H, Sternberg J B, Ovchinnikov SY and Briggs J S 2010 *Phys. Rev. Lett.* **104** 033201

[5] Chen Z J, Liang Y Q and Lin C D 2010 *Phys. Rev. Lett.* **104** 253201

[6] Zhou L X, Yan Y G and Men F D 2010 *Chin. Phys.* B **19** 073401

[7] Yan S, Ma X, Zhang P, Xu S, Zhang S F, Zhu X L, Feng W T and Liu H P 2011 *J. Phys.* B: *At. Mol. Opt. Phys.* **44** 055202

[8] Nixon K L and Murray A J 2011 *Phys. Rev. Lett.* **106** 123201

[9] Chen Z B, Yang H, Wu X J and Zhang S M 2011 *Acta Phys. Sin.* **60** 063402 (in Chinese)

[10] Ren X G, Senftleben A, Pflüger T, Dorn A, Bartschat K and Ullrich J 2010 *J. Phys.* B: *At. Mol. Opt. Phys.* **430** 35202

[11] Staicu C E M, Catoire F, Naja A, Ren X G, Lahmam-Bennani A, Nekkab M, Dal Cappello C, Bartschat K and Whelan C T 2007 *J. Electron Spectrosc. Relat. Phenom.* **161** 27

[12] Duguet A, Lahman-Bennani A, Lecas M and Ei Marji B 1998 *Rev. Sci. Instrum.* **69** 3524

[13] Lahmam-Bennani A 2002 *J. Electron Spectrosc. Relat. Phenom.* **123** 365

[14] Yang H, Zhang S M and Wu X J 2009 *Acta Phys. Sin.* **58** 6938 (in Chinese)

[15] Hu X Y and Zhou Y J 2010 *Acta Phys. Sin.* **59** 2423 (in Chinese)

[16] Dürr M, Dimopoulou C, Dorn A, Najjari B, Bray I, Fursa D V, Chen Z J, Madison D H, Bartschat K and Ullrich J 2006 *J. Phys.* B: *At. Mol. Opt. Phys.* **39** 4097

[17] Colgan J, Foster M, Pindzola M S, Bray I, Stelbovics A T and Fursa D V 2009 *J. Phys.* B: *At. Mol. Opt. Phys.* **42** 145002

[18] Whelan C T, Allan R J, Rasch J, Walters H R J, Zhang X, Roder J, Jung K and Ehrhardt H 1994 *Phys. Rev.* A **50** 4394

[19] Ward S J and Macek J H 1994 *Phys. Rev.* A **49** 1049

[20] Gianturco F A and Rodriguez-Ruiz J A 1993 *Phys. Rev.* A **47** 1075

[21] de Fazio D, Gianturco F A, Rodriguez-Ruiz J A, Tang K T and Toennies J P 1994 *J. Phys.* B: *At. Mol. Opt. Phys.* **27** 303